Turbulence intensity levels were calculated by dividing the root-mean-square (rms) of the velocities measured with DFLDA by the mean DFLDA-velocity at each run. These values are biased by the fluctuations of the true airspeed during a run. TAS fluctuation levels did not differ significantly during the measurements as was checked with the ADC. Taking account of the bias due to fluctuations of TAS of the aircraft, the turbulence levels measured in the boundary layer seem reasonable.

The difference between the TAS measured with the ADC of the aircraft and the velocities determined with DFLDA at the maximum distance from the glass plate (position = 94 mm) was calculated at 128, 177, and 240 kt true airspeed. The maximum deviation was 2.6% at 240 kt. Such small differences may be expected, because the flow in the mcv is influenced by the presence of the aircraft.

Data rates were typically 20–250 Hz, and the data points shown in Fig. 2 were typically averaged over 2000–8000 individual velocity measurements.

Measurements Outside of Clouds

In general, it is considered preferable to measure outside of clouds for two reasons. First, clouds are not always available. Second, the scattering centers are water droplets which have a wide size distribution, much of which lies above the 0.5–1 μm limit, under which the particles truly follow the flow around the aircraft at cruising speeds.

Outside of clouds the data rate decreased considerably, typically less than 1 Hz. However, observation of the signals from the detector on an on-board oscilloscope indicated that a significantly higher number of particles was present, but signals were apparently not of sufficient quality to be validated by the counter processor. Future measurements should therefore employ frequency domain processors, which offer better detection schemes no longer based on amplitude discrimination, as well as more robust frequency estimators less sensitive to signal noise. A shorter focal length, e.g., 60 mm instead of 120 mm, can also be used to increase the particle detection probability. The traversing range is more limited with the shorter focal length lens.

Conclusions

The results of this study indicate that in-flight LDA measurements are now feasible. Velocity measurements in the boundary layer were obtained. The results indicate the boundary-layer thickness and would certainly also indicate separation and/or recirculating flow features if present. Therefore, the LDA technique may find increasing application for in-flight aerodynamic studies.

Flexibility in operation, robustness of laser and probe, and especially the low power consumption, make the DFLDA attractive for in-flight applications compared with other laser Doppler anemometers. Further improvements of both the optical system and the signal processing system can be expected. For instance, Nd:Yag lasers, which will be available in the near future with output powers of up to 1 W are an attractive alternative to the laser diodes. The size of these lasers does not exceed the size of the diode laser used in the present study. Also, with some frequency mixing, it may be possible to employ more efficient signal processors to improve the signal validation rate.

References

[1]Durst, F., Melling, A., and Whitelaw, J. H., "Principles and Practice of Laser-Doppler Anemometry," 2nd ed., Academic Press, London, 1981.

[2]Stieglmeier, M., and Tropea, C., "Mobile Fiber-Optic Laser Doppler Anemometer," *Applied Optics*, Vol. 31, No. 21, 1992, pp. 4096–4105.

Aircraft Landing Gear Positioning Concerning Abnormal Landing Cases

Hsing-Juin Lee*
National Chung-Hsing University, Taichung, Taiwan 40227, Republic of China
and
Cheng-Yi Chiou†
Chung Shan Institute of Science and Technology, Taichung, Taiwan 40227, Republic of China

Introduction

AIRCRAFT landing gear mechanisms serve several design purposes such as supporting the weight of aircraft, providing rolling chassis/taxiing, and shock absorption function, especially during takeoff and landing.[1,2] Out of many thousands of landings during the lifecyle of a typical aircraft, there might be some abnormal landings due to various causes such as adverse weather. For a typical normal landing of an airplane, once the main landing gears (MLG) touch down first, the pilot will operate the pitch controls to provide proper aerodynamic righting moment in order to avoid heavy nose landing gear (NLG) impact on the runway which may cause probable damage or serious accidents. However, this kind of aerodynamic righting moment may not work in time, especially under adverse weather conditions such as wind shear, therefore, it cannot be counted on in many cases of abnormal landings.

The NLG and MLG together share the ground sinking impact energy for an airplane at landing. The landing approach is subject to pilot skill, airplane damage conditions (after combat), runway situations, and weather conditions. Sometimes the NLG may touch down first abnormally, or free-fall to the ground without correct pitch control for tail down landing. In these cases, the NLG will absorb more sinking energy than the usual amount. For normal landing, the sinking speed generally falls in the category of 0.3 m/s (≈1 fps) to 0.915 m/s (≈3 fps). Any landings with sinking speed above 2.44 m/s (≈8 fps) are commonly considered a very hard landing,[3] a landing that hard might occur only once in 300 landings for military service. Due to probable various abnormal landing conditions, the landing gear design is required to allow for a wide range of sinking speed. Hence, as stated in military specification MIL-A-8862A,[4] usually landing gear structural requirements for limit load are 3.048 m/s (10 fps) for land-based fighter airplane and 3.96 m/s (≈13 fps) for trainer or other special types such as carrier-based naval fighter airplanes.

The layout and design of aircraft landing gears is a rather complicated iterative process for engineering judgements and compromises.[5] The proper positioning of aircraft landing gears is particularly important to pursue an optimal c.g. location and weight distribution between NLG and MLG, statically speaking. Usually, the NLG is designed to carry 6–20% of the total weight of an aircraft. Despite all the traditional prudent design consideration for aircraft landing gears, the search for dynamically superior positioning of aircraft landing gears has not been well addressed in terms of percussion theory as reflected by current literature.[1,6–8] In this study, the concept of center of percussion (Cp), center of oscillation (Co), and

Received Aug. 17, 1992; revision received Feb. 8, 1993; accepted for publication Feb. 16, 1993.

*Associate Professor of Mechanical Engineering, National Chung-Hsing University. Member AIAA.

†Assistant Researcher, Aeronautical Research Laboratory.

associated interchangeability property will be reviewed first, then this percussion theory will be used to introduce the unique concept of dynamically equivalent lumping mass concept. Subsequently, these ideas are merged with the angular momentum analysis of the aircraft to obtain ingenious equations for the proper apportioning of sinking energy between the NLG and MLG for possible abnormal landings during aircraft lifetime. If the concept presented in this study can be employed prudently for positioning the aircraft landing gears, then the lifetime accident risk for the relatively fragile nose gear will be reduced.

Preliminary Review of the Percussion Theory

In an attempt to apply the percussion theory later for positioning of aircraft landing gears, the basic percussion theory is briefly reviewed here. A typical rigid bar with known mass m, the c.g., and mass moment of inertia about c.g. (I_{cg}) is shown in Fig. 1. Any point on such a bar can be designated as Co; corresponding to this point a specific point on the bar called Cp can be found. While an external impulsive force P is acting on the special point Cp (Fig. 1), there will be no horizontal acceleration for the Co point at the instant of impact. Therefore, if Co is pivotally supported, there will be no force acting on the pivotal support at that moment. The Cp corresponding to a designated Co can be found by the following procedures.

For a impact force P acting at point A (Fig. 1), two forces P_2 and P_3 with the same magnitude of P and mutually opposite directions are added at c.g. For such a rigid body, the dynamics behavior is unchanged under this circumstance, thus the bar can be thought as subject to a force P_2 at c.g. and a clockwise couple $[P(q_0 - r_0)]$. Due to the P_2 force alone, the said bar will have a purely translational acceleration $\ddot{X}$ to the left

$$\ddot{X} = (P/m) \tag{1}$$

In order to have an appropriate angular acceleration $\ddot{\theta}$ for the bar to counteract the translational acceleration at point Co, the $\ddot{\theta}$ should be

$$\ddot{\theta} = (\ddot{X}/r_0) = (P/mr_0) \tag{2}$$

where r_0 is the distance between the points Co and c.g. Then by the moment-angular acceleration equation

$$P(q_0 - r_0) = I_{cg}(P/mr_0) \tag{3}$$

where q_0 is the not yet known distance between Co and the Cp to be found. After rearranging terms, q_0 can be expressed as

$$q_0 = \frac{I_{cg} + mr_0^2}{mr_0} = \frac{I_0}{mr_0} = \frac{mk_0^2}{mr_0} \tag{4}$$

or

$$q_0 = (k_0^2/r_0) \tag{5}$$

where I_0 is the mass moment of inertia about Co, and k_0 is the radius of gyration about Co. With known inertia properties of the bar and designated center of oscillation, the corresponding center of percussion can be easily found by Eq. (5). Conversely, if the original Cp point A in Fig. 1 is taken as the new center of oscillation, then by Eq. (5), the new corresponding Cp distance (q_1) from the newly designated Co point can be expressed as

$$q_1 = \frac{k_1^2}{r_1} = \frac{mk_1^2}{mr_1} = \frac{I_A}{mr_1} \tag{6}$$

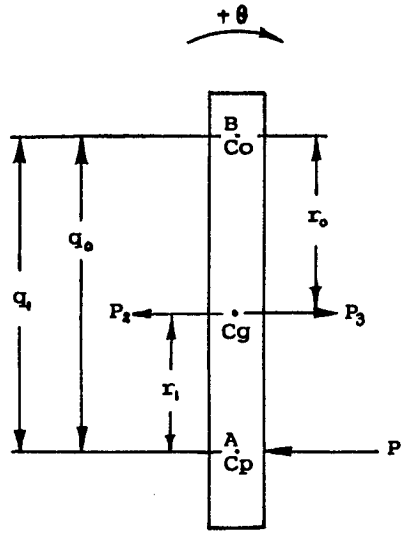

Fig. 1 Illustration for reviewing percussion theory.

where k_1 is the radius of gyration of the bar about the new Co (point A), r_1 is the distance between points A and unchanged c.g., and I_A is the mass moment of inertia about the point A. Equation (6) can be further processed by applying the transfer principles for mass moment of inertia between parallel axes

$$q_1 = \frac{I_A}{mr_1} = \frac{(mk_0^2 - mr_0^2) + m(q_0 - r_0)^2}{m(q_0 - r_0)}$$

$$= \frac{k_0^2 - r_0^2 + q_0^2 + r_0^2 - 2q_0r_0}{q_0 - r_0} = q_0 \tag{7}$$

This proves that the Co and its corresponding Cp are interchangeable. Its physical meaning will become more clear with the aid of lumping mass concept in the next section.

Percussion Theory for Positioning Aircraft Landing Gears

On the other hand, Eq. (3) can be processed differently as

$$(q_0 - r_0)r_0 = (I_{cg}/m) = k_{cg}^2 \tag{8}$$

where m is the mass of airplane, also let $(q_0 - r_0) = l_1$ and $r_0 = l_2$ as shown in Fig. 2a, then Eq. (8) can be written as

$$l_1l_2 = k_{cg}^2 \tag{9}$$

where the k_{cg} is the radius of gyration about the c.g. of the airplane. This is an equation similar to Eq. (5), but in a different format. The points A and B shown in Fig. 2a are the Cp and Co interchangeably. The distance between A and B can be designated as

$$l = l_1 + l_2 \tag{10}$$

In fact, Eq. (9) reveals important physical meaning of dynamically equivalent lumping masses, i.e., while the mass of the rigid bar is lumped at points A and B, respectively, according to the following apportioning:

$$m_1 = \frac{l_2}{l_1 + l_2} m = \frac{l_2}{l} m \tag{11}$$

$$m_2 = \frac{l_1}{l_1 + l_2} m = \frac{l_1}{l} m \tag{12}$$

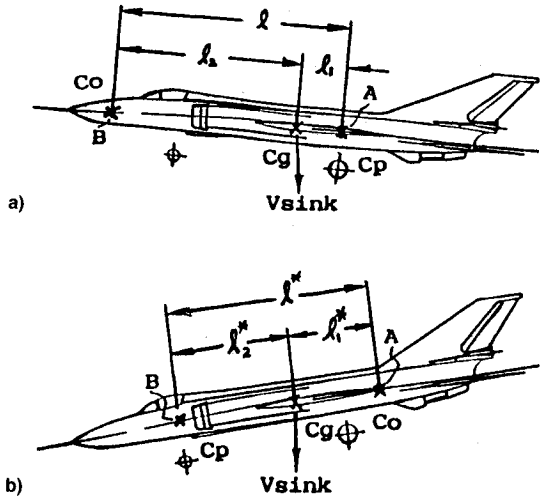

Fig. 2 Aircraft landings with a) a normal landing and b) an abnormal landing.

then the m_1 and m_2 with massless link can replace the original rigid bar in a dynamically equivalent sense. This assertion can be directly proved by solving the following three condition equations for dynamical equivalence for given m, l_1, c.g. position, and k_{cg}:

$$m_1 + m_2 = m \tag{13}$$

$$m_1 l_1 = m_2 l_2 \tag{14}$$

$$m_1 l_1^2 + m_2 l_2^2 = I_{cg} = m k_{cg}^2 \tag{15}$$

The three unknowns are obtained as

$$l_2 = k_{cg}^2 / l_1 \tag{16}$$

$$m_1 = (l_2/l)m \tag{17}$$

$$m_2 = (l_1/l)m \tag{18}$$

Note that Eq. (16) is corresponding to Eq. (9), in that light the physical meanings of Co, Cp, and associated interchangeability can be understood in a more clear silhouette. A typical aircraft at normal landing is shown in Fig. 2a, since the angle θ between the fuselage and the runway horizon is generally small, for simplicity in discussion any length quantity multiplied by cos θ can be considered unchanged. At the onset of landing, the sinking speed of the airplane can be largely taken as constant due to the delicate balance of various external forces at this moment. For such a normal landing, the main gears are supposed to touch down on the runway first. The total sinking energy of the airplane to be absorbed by MLG is

$$K_E = \tfrac{1}{2} m_1 (V_{sink})^2 \tag{19}$$

where (V_{sink}) is the sinking speed of airplane. The airplane can be simulated primarily as a rigid bar (Fig. 2a). In that case, by the principle of conservation of angular momentum, the angular velocity ω of the fuselage after touchdown of the MLG can be expressed as

$$I_A \omega = (m V_{sink}) l_1 \tag{20}$$

where l_1 is the distance between c.g. and the MLG along the fuselage. Then

$$\omega = (m V_{sink} l_1)/I_A \tag{21}$$

by Eq. (4)

$$\omega = \frac{m V_{sink} l_1}{m l l_1} = \frac{V_{sink}}{l} \tag{22}$$

where l is the (Cp-Co) distance corresponding to the (Cp-c.g.) distance l_1, it is worthwhile to note that these length quantities, together with the position of c.g., the total mass, and the mass moment of inertia about c.g., are all time-dependent functions. They depend on the fuel storage allocation and consumption management, the passenger/cargo allocation situation, and the weaponry attached or fired in the cases of military aircraft. Referring back to Eq. (20), multiplying both sides by $(\omega/2)$

$$\frac{1}{2} I_A \omega^2 = \frac{1}{2} m V_{sink}(l_1 \omega) = \frac{1}{2} m V_{sink}(l\omega) \left(\frac{l_1}{l}\right) = \frac{1}{2} \left(\frac{l_1}{l} m\right) V_{sink}^2 \tag{23}$$

The above equation gives the maximal possible amount of sinking energy left for the NLG to absorb after the MLG has touched down first (assuming it is still without the instant pitch control operation).

On the other hand, during the lifetime of a typical aircraft, a particular aircraft stands a good chance to experience some abnormal landings, no matter whether it is due to adverse weather causes (such as gust or wind shears), difficulties for landings on aircraft-carrier at bad sea, or due to various mechanical/electrical and other possible causes. One important category of abnormal-attitude landing cases is that the NLG touches down first at landing. In that case, the NLG becomes the new Cp for the airplane as a whole, also the new distance l_2^* between the NLG and the c.g. becomes the dominating (Cp-c.g.) distance for finding the new Co and the new (c.g.-Co) distance l_1^* (Fig. 2b). Under this situation, by Eq. (23), the NLG has to absorb an amount of sinking energy at least equal to

$$\frac{1}{2} \left(\frac{l_1^*}{l^*} m\right) V_{sink}^2 \tag{24}$$

For a simple numerical example in nondimensional form, giving that

$$l_1 = 1, \qquad l_2 = 10, \qquad l_2^* = 0.8 l_2 \tag{25}$$

therefore

$$l_1^* = 1.25 l_1$$

Substituting these quantities into Eqs. (23) and (24) and comparing the results, it can be easily seen that in the case of a nose-down landing with only slightly shorter l_2^* as given above, the NLG could absorb an amount of sinking energy 50% higher than that of a normal landing.

Conclusion

In this study, the search for dynamically superior positioning of aircraft landing gears has been addressed. The percussion theory and lumping mass concept are merged with the angular moment analysis to obtain Eqs. (23) and (24) for assessing the amount of sinking energy absorbed by NLG for normal and abnormal landing cases, respectively. It can be easily seen that even a slightly closer positioning of NLG to c.g. can abruptly increase the sinking energy absorbed by the NLG in some abnormal landing cases. If NLG and MLG can be designed at Co and Cp locales mutually and interchangeably according to Eq. (9), then the NLG will absorb a definite percentage of sinking energy, no matter for normal or abnormal attitude landings as shown in Fig. 2. While the above concept is employed prudently, the lifetime accident risk for the relatively fragile nose gear can be reduced.

Aircraft design is well known as a complicated compromising process, although the above theoretical analysis need not be considered as a dictating factor in the exact layout of an aircraft, its significance with special attention to Eq. (9) should be properly weighted in a well-rounded design or cargo/fuel disposition management for existing aircraft. Incidentally, the NLG should not be positioned too far forward from the c.g. of an aircraft to overprotect the NLG for abnormal landings, since too light a load on NLG will give an adverse effect to the steering capability and righting moment for the aircraft in risky drift landings. For aircraft, all the mass, the c.g. locale, the radius of gyration, and Co/Cp locales all are variables, obviously the sinking energy absorbed by the NLG is very sensitive to these variables whose volatility and sensitivity may have to be considered prudently to achieve an optimal overall design compromise in a probabilistic sense.

References

[1]Currey, N. S., "Aircraft Landing Gear Design: Principles and Practices," AIAA Education Series, AIAA, Washington, DC, 1988, pp. 1–67.

[2]Conway, H. G., "Landing Gear Design," Chapman Hall, London, 1958.

[3]"MIL-L-8552: Shock Absorber—AFSC and USN," U.S. Air Force, Military Specification, Wright-Patterson AFB, OH, 1968, pp. 3–6.

[4]"MIL-L-8862: Airplane Strength and Rigidity, Landing and Ground Handling Loads," U.S. Air Force, Military Specification, Wright-Patterson AFB, OH, 1971, pp. 1–26.

[5]Darlington, D. R. F., "Landing Gear—A Complete System Approach," Vertiflite, American Helicopter Society, March/April 1987.

[6]Stinton, D., "The Anatomy of the Aeroplane," BSP Professional Books, Palo Alto, CA, 1987, pp. 170–176.

[7]Ohly, B., "Landing Gear Design—Contemporary Views and Future Trends," *International Journal of Aviation Safety*, March 1985, pp. 6–10.

[8]Young, D. W., "Aircraft Landing Gears—The Past, Present and Future," *Proceedings of the Institution of Mechanical Engineers*, Vol. 200, No. D2, 1986, pp. 75–92.

Joined-Wing Model Vibrations Using PC-Based Modal Testing and Finite Element Analysis

Benhe Qu* and Malcolm A. Cutchins†
Auburn University, Auburn, Alabama 36849

Introduction

In recent years with the popularity of personal computers, experimental modal analysis has been greatly enhanced with the advances and development of PC-based fast Fourier transform (FFT) analyzers. When equipped with well designed and user-oriented modal analysis software, the analyzer-in-a-portable-PC provides a powerful and convenient method for studying practical structural vibration problems. In addition, in an educational environment, the portability feature of the modal system gives unique opportunities for presenting modal testing and mode animation in the university classroom.[1] Primary emphasis here, however, centers on the test and analysis comparison for a joined-wing vibration model. With a COMPAQ PORTABLE 386® personal computer, an impulse hammer and associated instrumentation, a joined-wing model is employed as a specimen in a modal testing experiment. The structural dynamic behavior of the joined-wing model is obtained and compared with MSC/NASTRAN analysis results. The aerodynamics of the joined-wing concept have been thoroughly overviewed by its inventor.[2]

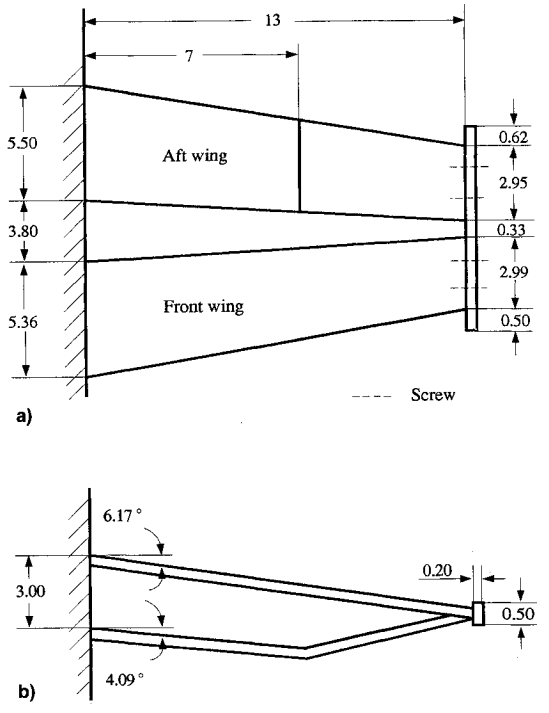

Fig. 1 Geometry of the joined-wing model (units in inches): a) planform view and b) front view.

A joined-wing airplane is defined as an airplane that incorporates tandem wings arranged to form diamond shapes in both plan and front views. The aerodynamics of the joined-wing have been studied by several individuals, but there is no literature dealing with its structural dynamics found to date. This work is an outgrowth of a variation of the typical joined-wing, but emphasis is on the structural dynamics, not the aerodynamics. The roots of each of the airfoils which make up the joined-wing of this work meet with the fuselage (as opposed to the typical joined-wing which has one wing attached to the fuselage and one attached to the tail of the aircraft). The aerodynamics of such an arrangement have been studied at Auburn University by Burkhalter et al.[3] including a wind-tunnel experimental model. The vibration model of this effort[4] has been based on their wind-tunnel model, but it was not intended to be an accurately scaled model due to the high cost of building such a model.

The geometry of the joined-wing model is shown in Figs. 1a and 1b. The model is for the left side of the aircraft. It consists of two wings in which the aft wing with anhedral from the bottom of the fuselage is swept forward and bent up near the middle of the span, to join the forward wing which is swept back with anhedral from the top of the fuselage. A joining beam connects the forward wing and the aft wing together by four screws at the tips. Both the forward and aft wings are fixed to an aluminum plate by bolts at the roots.

Received Feb. 18, 1992; presented as Paper 92-2260 at the AIAA/ASME/ASCE/AHS/ASC Structures, Structural Dynamics and Materials Conference, Dallas, TX, April 13–15, 1992; revision received Jan. 4, 1993; accepted for publication Jan. 11, 1993.

*P & W Scholar, 1990–91, Pratt & Whitney of China, Inc., Department of Aerospace Engineering; currently a Ph.D. Candidate at Pennsylvania State University, University Park, PA 16802.

†Professor, Department of Aerospace Engineering. Associate Fellow AIAA.